Decision-Making in Physical Intelligent Systems Regulated by Growth Rate Factors

Till D. Frank[1]

[1] CESPA, Department of Psychology, University of Connecticut, Storrs, USA

Correspondence: Till D. Frank, CESPA, Department of Psychology, University of Connecticut, 406 Babbidge Road, Storrs, CT, 06269, USA. Tel: 1-860-486-3906. E-mail: till.frank@uconn.edu

Abstract

In the literature, self-organizing physical and chemical systems have been proposed as candidates for physical intelligent systems that may solve problems in the field of artificial intelligent in a non-algorithmic way that is not based on computation. In this theoretical study, decision-making in such physical intelligent systems is discussed in terms of non-equilibrium transitions between two self-organized states. The control parameter driving the non-equilibrium transitions is related to two growth rate factors. It is shown for a particular non-equilibrium system that the decision-making process satisfies the principle of selecting the state with the fastest growth rate factor. The system under consideration is a two component gas discharge system whose current flows can be described by means of an electronic blueprint.

Keywords: physical intelligence, decision-making, bifurcation theory, selection principle, growth rates, 4th law

1. Introduction

It has been proposed that physical and chemical self-organizing systems may exhibit problem-solving abilities similar to humans and animals (Jun & Hübler, 2005; Hübler, 2009; Turvey & Carello, 2012). In this context, the phrase "physical intelligent systems" has been coined. In particular, in engineering applications the motivation for studying physical systems solving problems in the field of artificial intelligence (e.g., Isa et al., 2008; Adenowo & Patel, 2014) is to explore alternatives to algorithmic, computer-based intelligence. Such alternatives may help to overcome limitations of the state-of-the-art computer technology. Pattern formation systems are promising candidate systems for physical intelligence (Frank, 2011a, 2012a). In particular, associative memory systems may be based on gas or fluid systems that exhibit roll patterns when driving into a Benard instability (Bestehorn & Haken, 1991; Haken, 1991). Decision making systems may be realized by means of pattern formation systems, as well. This idea has been exemplified for an internet router storage buffer (Frank, 2011b). One of the most fundamental type of decision making systems are systems switching between two possible states (binary decision making). In this context, the question arises whether or not there are general principles that govern decision making in self-organizing physical systems. At least two principles have been considered that view decisions as non-equilibrium phase transitions in far-from equilibrium systems or bifurcations in dynamical systems. The so-called 4th law states that non-equilibrium phase transitions in physical systems happen in such a way that the speed (rate) at which entropy is produced is maximized (Swenson & Turvey, 1991). The principles of fastest growth rates states that in dynamical systems bifurcations from a self-organized state A to a self-organized state B happen such that the growth rate parameter of the emerging state B is higher than the growth rate of the state A. The latter principle has rigorously been derived for systems satisfying Haken's pattern formation amplitude equations (Frank, 2011b, 2011c, 2012b) and for the competitive Lotka-Volterra model (Frank, in press). The two principles are related to each other. It has been advocated that in a large class of systems the growth rate parameters are measures for the speed of entropy production (Frank, 2010, 2011b). Therefore, for such systems the selection principles of fastest growth rates is consistent with the aforementioned 4th law.

As mentioned above, the principle of fastest growth rates governs mode-mode transitions in pattern formation systems satisfying Haken's amplitude equations and determines bifurcations in dynamical systems described by the competitive Lotka-Volterra model. In the search for physical intelligence, physical systems exhibiting such mode-mode transitions and bifurcations may be used as smart decision making devices (recall the

abovementioned example of an internet router). We show in what follows that a two compartment gas discharge system with compartments L (left) and R (right) exhibits hysteretic transitions between the emergence of gas discharge solitons in the compartments L and R. That is, a soliton existing in compartment L disappears and a soliton in compartment R emerges or vice versa. The control parameter involved in these transitions is an asymmetry parameter. The transition is similar to human decision making transitions in object grasping. Small objects are typically grasped with one hand, while larger objects are grasped with two hands. Laboratory experiments have confirmed the hysteretic nature of such grasping transitions related to two-choice decision making (Richardson et al., 2007; Lopresti-Goodman et al. 2009). In analogy to human grasping behaviour guided by object-size perception, we will argue that the two compartment gas discharge system can recognize or perceive the asymmetry between the compartments and can be regarded as a physical, decision making device regulated by that asymmetry parameter. Most importantly, we will show that the transitions (decisions) satisfy the principle of fastest growth rates

2. Decision Making Regulated by Growth Rate Factors

2.1 Current Flow Description of a Two Compartment Gas Discharge System

The study of gas discharge systems is of importance for industrial and entertainment applications. In addition, gas discharge systems are a testbed for studying pattern formation in nonlinear far-from equilibrium systems. Typically a gas discharge system consists of a gas filled chamber between two electrodes. A constant voltage U_0 is applied across the gap. For sufficiently large values of U_0 discharge solitons can be observed (see e.g. Bödeker et al., 2003,2004) and the reviews by Purwins et al. (2010) and Liehr (2013)). Let us consider rectangular electrodes such that the discharge gap forms a cuboid with a long axis and two short axes. Along the long axis, solitons can emerge at any position provided U_0 is high enough. For our purposes, it is important to notice that the current flows in the device can be described by means of an electronic blueprint involving resistors, capacitors, and inductors (Purwins et al., 2010). To this end, the long axis is compartmentalized into cells or compartments. That is, we consider a coarse-grained description in which all solitons that emerge in a certain "bin" are considered to belong to the same equivalent class. In other words, they represent the same soliton. The simplest arrangement that allows for a discussion of physical intelligence is a gas discharge device that is described in terms of two compartments. Even in this case the original electronic blueprint yields a description that is mathematically involved. However, this original blueprint includes a 5 piece core circuit shown in Figure 1.
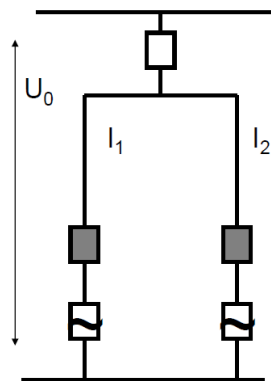

Figure 1. A five piece core model describing the current flows across the discharge gap of a two compartment gas discharge system. The model is composed of a linear ohmic resistor (empty box, top part), two inductors (grey boxes) and two nonlinear resistors (empty boxes marked with a tilde)

As we will show below this core model is sufficient to describe the multistable (here bistable) nature of gas discharge systems. In this context, we note that a state with a relative high current in one compartment but a relative low current in the other compartment reflects that the gas discharge system exhibits only one soliton. The soliton is located in the high current compartment. As such, for a two compartment model there are four different states. Both compartments do not exhibit a soliton. Only the left compartment exhibits a soliton. Only the right compartment exhibits a soliton. Both compartments exhibit solitons.

The first objective is to explain the experimentally observed multistability (here bistability) of gas discharge

systems in terms of a multistability (bistability) of the underlying current flow model. The second objective is to use the model to show that gas discharge systems can recognize asymmetries. That is, they can be regulated by asymmetries such that transitions occur between the two states in which only one compartment exhibits a soliton. The two states that involve a single solitons may be considered as two possible decisions in a two-choice situation (e.g. a "yes" or "no" decision). In this sense, the gas discharge model may be interpreted as a physical decision-making devise.

2.2 Dynamical Systems Modelling

Let us derive the evolution equations for the currents flowing through the left and right branches of the two compartments core model. The voltage U_0 can be computed from the voltages U_{top} and $U_{bottom,k}$ across the top and bottom circuit of the device such that

$$U_0 = U_{top} + U_{bottom,k} \tag{1}$$

Note that with the index k=1,2 we distinguish between the left (k=1) and right (k=2) compartments. The total current in the top circuit is given by the sum of the currents I_k of the two compartments: $I(tot)=I_1+I_2$. The voltage U_{top} follows Ohm's law such that

$$U_{top} = R \cdot I(tot) = R\left(I_1 + I_2\right) \tag{2}$$

The inductors are assumed to have the same inductivity L such that the voltages $U_{L,k}$ at the inductors is given by

$$U_{L,k} = L \cdot \frac{d}{dt} I_k \tag{3}$$

The voltage-current relationship of the nonlinear resistors in the bottom circuits are approximately described by cubic functions like (see Figure 2a in Purwins et al. (2010))

$$U_{NL,k}(I_k) = \delta_k + U* + b\left[\left(I_k - s\right)^3 - \left(I_k - s\right)\right]$$
$$U* = b(s^3 - s) \tag{4}$$

with b,s>0. The parameters δ_k capture impurities (inhomogeneities) leading to asymmetric properties of the two nonlinear resistors. For $\delta_k =0$ and k=1,2 the resistors have the same properties and the two compartment gas discharge system is symmetric. For our purposes, it is sufficient to consider a single asymmetry parameter (rather than 2 independent parameters). Therefore, we put

$$\delta_k = (-1)^k \cdot \Lambda \tag{5}$$

For Λ=0 the resistors are identical and the gas discharge system exhibits symmetry. For $\Lambda{\neq}0$ the nonlinear resistors have slightly different properties and we are concerned with an asymmetric gas discharge device. We refer to Λ as effective asymmetry parameter. The voltages in the bottom circuits are given by

$$U_{bottom,k} = U_{L,k} + U_{NL,k} \tag{6}$$

Substituting these relations in the equation for voltage U_0, we obtain

$$U_0 = U_{top} + U_{L,k} + U_{NL,k}(I_k)$$
$$= R \sum_{m=1,2} I_m + L \frac{d}{dt} I_k + U_{NL,k}(I_k) \tag{7}$$

for k=1,2. Solving for I_k , we obtain two coupled first order differential equation in terms of

$$L \frac{d}{dt} I_k = U_0 - U_{NL,k}(I_k) - R \sum_{m=1,2} I_m \tag{8}$$

with k=1,2. Rescaling time, we can eliminate the inductivity L such that

$$\frac{d}{dt} I_k = U_0 - U_{NL,k}(I_k) - R \sum_{m=1,2} I_m \tag{9}$$

More explicitly, we have

$$\frac{d}{dt} I_k = U_0 - \delta_k - U* - b\left[(I_k - s)^3 - (I_k - s)\right] - R \sum_{m=1,2} I_m \tag{10}$$

2.3 Global Stability and Gradient Dynamics

The dynamical model can be expressed by means of a gradient dynamics involving a potential. That is, we have

$$\frac{d}{dt} I_k = -\frac{\partial V}{\partial I_k}$$

$$V = -(U_0 - \delta) \sum_{m=1,2} I_m - \sum_{m=1,2} \Phi(I_m) + \frac{R}{2}\left(\sum_{m=1,2} I_m\right)^2 \tag{11}$$

with

$$\Phi(z) = -\int^{z} U_{NL}(z') dz' \tag{12}$$

The term $-U_{NL}$ in the evolution equations for the currents reflects a globally attractive force. Therefore, $-\Phi$ is a globally attractive potential. The last term on the right hand side of the potential V reflects a globally attractive component. It is quadratic and dominates the linear, first term of the potential for large currents. Therefore, V is a globally attractive potential. This implies that for any initial currents $I_1(t=0)>0$ and $I_2(t=0)>0$ in the two gas discharge compartments, the gas discharge system will evolve in time such that the currents will converge to fixed point values. In other words, the gas discharge system will become stationary in any case.

2.4 Unstable Co-Existence Fixed Point

In order to identify a bistable parameter domain exhibiting two stable winner-takes-all fixed points and one unstable co-existence fixed point, we focus on the symmetric case and conduct some analytical computations. For the symmetric case, the co-existence fixed point is assumed to have coordinates $I_1=I_2=\xi$. Note that at this stage of our analysis the precise value of ξ is unknown. Let ε_k denote small deviations from the fixed points coordinates such that $I_1(t)= \xi+\varepsilon_1(t)$ and that $I_2(t)= \xi+\varepsilon_2(t)$. Substituting these relations into the evolution equations for the currents and conducting a linear stability analysis, we obtain

$$\frac{d}{dt} \varepsilon_k = b\left[1 - 3(\xi - s)^2\right]\varepsilon_k - R \sum_{m=1,2} \varepsilon_m \tag{13}$$

for k=1,2. This equation can equivalently be expressed as

$$\frac{d}{dt} \varepsilon_1 = A\varepsilon_1 - R\varepsilon_2$$

$$\frac{d}{dt} \varepsilon_2 = -R\varepsilon_1 + A\varepsilon_2 \tag{14}$$

and

$$A = b\left[1 - 3(\xi - s)^2\right] - R \tag{15}$$

The eigenvalues or Lyapunov exponents (Margaris, 2012) may be computed from the matrix involved in the equation above. Alternatively, we consider the evolution equations for the auxiliary variables $u(t)=\varepsilon_1(t)-\varepsilon_2(t)$ and $v(t)=\varepsilon_1(t)+\varepsilon_2(t)$, which read

$$\frac{d}{dt}u = (B - 2R)u$$

$$\frac{d}{dt}v = Bv$$

$$(16)$$

and

$$B = b\left[1 - 3(\xi - s)^2\right]$$

$$(17)$$

Consequently, if the co-existence point exists, then it is unstable if B>0 holds. Note that for B>0 we might have an unstable node or saddle. From the condition B>0 it follows

$$(\xi - s)^2 < \frac{1}{3}$$

$$(18)$$

Let us determine a parameter domain in which this sufficient condition for instability holds. To this end, we consider the case ξ=s. Substituting I_1=I_2=s into the evolution equations for I_k and putting the left-hand-sides equal to zero (stationary case), we obtain

$$U_0 - U^* = 2Rs$$

$$(19)$$

That is, if the voltage U_0 is appropriately chosen such that this matching condition is satisfied, then the co-existence fixed point I_1=I_2=s exist and is unstable.

2.5 Nullclines

Let us briefly describe the two nullclines of the two compartment gas discharge model. The nullcline dI_1 /dt=0 reads

$$R \cdot I_2(I_1) = U_0 - \delta_1 - U^* - b\left[(I_1 - s)^3 - (I_1 - s)\right] - R \cdot I_1$$

$$(20)$$

Likewise, the nullcline dI_2 /dt=0 reads

$$R \cdot I_1(I_2) = U_0 - \delta_2 - U^* - b\left[(I_2 - s)^3 - (I_2 - s)\right] - R \cdot I_2$$

$$(21)$$

In the symmetric case, that is, for δ_k=0 with k=1,2, the nullclines are symmetric with respect to the diagonal of the phase space spanned by I_1 and I_2. We obtain

$$I_2 = f(I_1) / R$$

$$I_1 = f(I_2) / R$$

$$(22)$$

with

$$f(z) = U_0 - U^* - b\left[(z - s)^3 - (z - s)\right] - R \cdot z$$

$$(23)$$

Both in the symmetric and the asymmetric case we see that nullclines are cubic functions in general. In fact, we need to exploit the cubic character of the functions in order to design a decision making device that involves a bistable dynamical regime in the symmetric case and exhibits hysteretic transitions in the asymmetric case, see Section 2.6 and 2.7.

2.6 Existence of a Bistable Parameter Domain for the Symmetric Two Compartment Gas Discharge System

Given the relative large parameter domain, we restrict ourselves to show the existence of at least one bistable parameter domain for the symmetric device (δ_k=0 for k=1,2). We conducted a numerical search taking the matching condition (19) into account. For fixed parameters s=2.0 and R=1.0 measured in arbitrary units (a.u.) we found that for b in [0.5,2] the nullclines had three intersection points provided that U_0 was chosen such that the matching condition U_0=U*+2Rs was satisfied. Figure 2 illustrates for a particular value of b the nullclines and the intersection points.

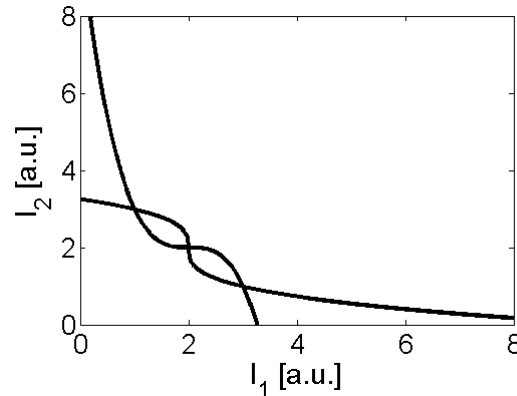Figure 2. Nullclines computed from Equations (22) and (23). Parameters: s=2.0, R=1.0, b=1.0, U_0 was defined by $U_0 = U^* + 2Rs$. The nullclines exhibit three intersection points. Topologically similar graphs were observed in the range $0.5 < b < 2$

As shown above the co-existence fixed point $I_1 = I_2 = s$ is unstable. In addition, due to the symmetry of the problem at hand, the two remaining fixed point have the same stability property. Since the device has global stability, we conclude that the two remaining fixed points are stable fixed points. In fact, we solved the evolution equations for the currents I_1 and I_2 numerically with initial conditions close to the two remaining fixed points. As expected we found that the solutions converged to the fixed points. The two stable fixed points describe a gas discharge systems with highly unequal current flows in the two compartments. For one of the stable fixed points we have a high current in compartment I and a low current in compartment II. For the other stable fixed points the opposite situation is true. As mentioned above, a relative high current reflects a gas discharge soliton in the respective compartment, whereas a low current indicates the absence of a soliton. That is, the fixed point with $I_1 > I_2$ indicates the presence of a soliton in compartment L only. Likewise, the fixed point with $I_2 > I_1$ indicates the presence of a soliton in compartment R only. For the conditions specified here, the voltage gap U_0 is large enough to induce the emergence of a gas discharge soliton. However, it is not sufficiently large to excite two solitons. As a result, a soliton appears either in compartment L or R. The gas discharge system is bistable. We will refer to the fixed points with $I_1 > I_2$ and with $I_2 > I_1$ as winner-takes-all fixed points because the soliton can be found in only one compartment. In summary, the nullcline analysis reveals the existence of a bistable parameter domain involving two stable fixed points and an unstable fixed point. The stable fixed points are winner-takes-all fixed points indicating the emergence of a soliton in one of the two compartments. The co-existence fixed point is unstable and therefore will not be observed in real devises that operate under finite temperature and are subjected to fluctuations.

2.7 Hysteretic Transitions and Decision Making Regulated by System Asymmetry

Next, let us take the asymmetry parameters device δ_k into consideration. As mentioned above, we focus on the effective asymmetry parameter Λ that induces via δ_k a positive and negative bias in the two compartments, see Equation (5). Since Λ affects the two compartments in the opposite way, it is plausible to assume that the two nullclines will be separated (pushed away from each other) when Λ is sufficiently large in the amount. In fact, calculating the nullclines for different values of Λ illustrates this effect, see Figures 3 and 4. In Figures 3 and 4 the top panels are identical with Figure 2 and serve as a reference point. That is, the top panels refer to the symmetric case with $\Lambda = 0$. The bottom panels illustrate the effect of $\Lambda \neq 0$. Figure 3 shows the impact of $\Lambda > 0$, which implies $-\delta_1 > 0$ (positive left bias) and $-\delta_2 < 0$ (negative right bias). Accordingly, the fixed point with $I_2 > I_1$ disappears and the gas discharge system becomes monostable. In this case, the system exhibits a soliton in compartment L and can not exhibit a soliton in compartment R. Figure 4 shows the impact of $\Lambda < 0$: the fixed point with $I_1 > I_2$ disappears and the gas discharge system becomes monostable again. In this case, the system exhibits a soliton in compartment R and can not exhibit a soliton in compartment L. As a result, the two compartment system can recognize or perceive the asymmetry. If the asymmetry is changed from a left biasing to a right biasing asymmetry then the soliton in the left compartment will disappear and a soliton in the right compartment will emerge. Likewise, if the asymmetry is changed in the opposite direction, the opposite bifurcation will be observed. This transition is hysteretic because the underlying system for $\Lambda = 0$ is bistable. In order to illustrate the hysteretic nature of the transition we changed the asymmetry parameter from the left biasing to the right biasing condition in three steps. For each step the evolution equations for the currents were

solved numerically. The trajectories are shown in Figure 5 (top panel). Likewise, we changed the asymmetry parameter from the right biasing to the left biasing condition in three steps and determined the current flow dynamics under this scenario by solving numerically the evolution equations for the currents. The result of the computer simulation is shown in Figure 5 (bottom panel). The transitions can be clearly seen in Figure 5. Moreover, the hysteretic nature is evident from comparison of the two panels of Figure 5.
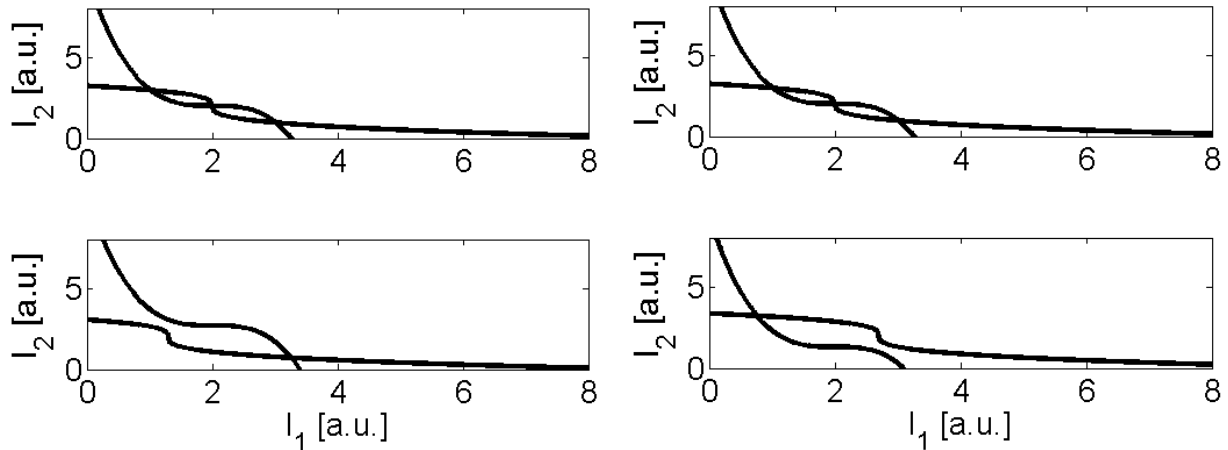
Figure 3. Top panel: nullclines for the symmetric case as in Figure 2. Bottom panel: nullclines for an asymmetric device. The nullclines were computed from Equations (20) and (21). Parameters: s=2.0, R=1.0, b=1.0. U_0 was defined by $U_0=U*+2Rs$. $\Lambda=0.7$, which implies for the negative asymmetry parameters: $(-\delta_1) = +0.7$ and $(-\delta_2) = -0.7$. Consequently, compartment L is positively biased, compartment R negatively biase

Figure 4. as in Figure 3 but for $\Lambda=-0.7$, which implies for the negative asymmetry parameters: $(-\delta_1) = -0.7$ and $(-\delta_2) = +0.7$. Consequently, compartment L is negatively biased, compartment R positively biased
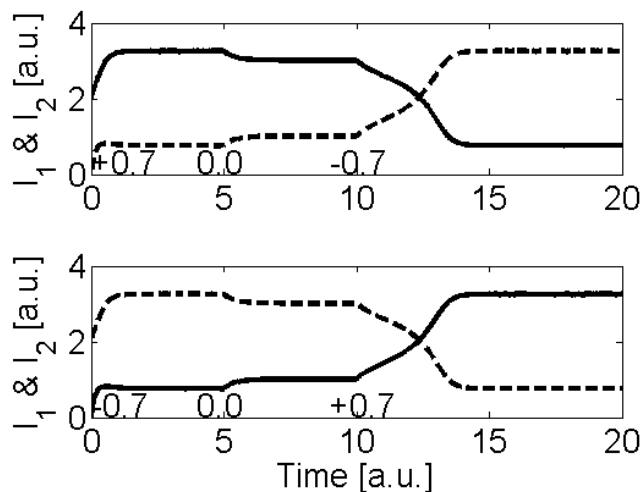
Figure 5. Simulation results showing trajectories $I_1(t)$ (solid lines) and $I_2(t)$ (dashed lines) computed from Equation (10) using an Euler forward method (single time step 0.01). Fixed parameters: s=2.0, R=1.0, b=1.0. U_0 was defined by $U_0=U*+2Rs$. Top panel: Λ was initially put at $\Lambda=+0.7$ (left bias). At t=5 time units Λ was put to $\Lambda=0$ (symmetric case). At t=10 time units Λ was put to $\Lambda=-0.7$ (right bias). Bottom panel: Λ was initially put at $\Lambda=-0.7$ (right bias). At t=5 time units Λ was put to $\Lambda=0$ (symmetric case). At t=10 time units Λ was put to $\Lambda=+0.7$ (left bias)

2.8 Selection Principle

The evolution equations for the currents in the gas discharge compartments involve in the lowest order additive terms. The additive terms result in an increase or decay of the currents that is linear with respect to time. We may consider the expression $\lambda_k = U_0 - \delta_k$ as an effective model parameter. For relative small asymmetry parameters (i.e., for $\delta_k < U_0$) the parameters λ_k can be interpreted as growth parameters. By means of these growth parameters, the evolution equations for the currents read

$$\frac{d}{dt}I_k = \lambda_k - U * - b\left[(I_k - s)^3 - (I_k - s)\right] - R\sum_{m=1,2}I_m \tag{24}$$

The hysteretic transition described in the previous section can be described by means of the growth rate parameters. If λ_1 is sufficiently large, then only the fixed point with $I_1 > I_2$ exists, (see Figure 3) and for any initial condition the gas discharge system will converge to that fixed point. A gas discharge soliton will emerge in the compartment I. Mathematically speaking, we define the threshold $\theta > 1$, whose precise value has to be determined numerically. For $\lambda_1 > \lambda_2 \cdot \theta$ the system is monostable. For $\lambda_1 < \lambda_2 \cdot \theta$ and $\lambda_2 < \lambda_1 \cdot \theta$ the system is bistable. If we change the ratio λ_1/λ_2 from a value $\lambda_1/\lambda_2 > \theta$ to a value $\lambda_1/\lambda_2 < \theta$ but $\lambda_1/\lambda_2 > 1/\theta$ then the system enters the bistability domain. The soliton in compartment I will continue to exist. For example, in the simulation illustrated in the top panel in Figure 5 the asymmetry parameter Λ was changed such that λ_1/λ_2 decreased from a value $\lambda_1/\lambda_2 > \theta$ to $\lambda_1/\lambda_2 = 1$. If the ratio λ_1/λ_2 is decreased further beyond the threshold $1/\theta$ then the system becomes monostable again. Only the fixed point $I_2 > I_1$ exists, (see Figure 4) and for any initial condition a gas discharge soliton will emerge in the compartment II. In particular, if λ_1/λ_2 is decreased beyond the threshold $1/\theta$ at transition from the fixed point with $I_1 > I_2$ to the fixed point $I_2 > I_1$ occurs (see Figure 5, top). The bifurcation takes place when λ_2 exceeds the threshold $\lambda_1 \cdot \theta$, that is, $\lambda_2 > \lambda_1$. The gas discharge system bifurcations to a new fixed point that exhibits a larger growth rate parameters. Likewise, if the ratio λ_1/λ_2 is increased from $\lambda_1/\lambda_2 < 1/\theta$ to a value $\lambda_1/\lambda_2 > \theta$ then a transition from the fixed point $I_2 > I_1$ to the fixed point $I_1 > I_2$ occurs (see Figure 5, bottom). Again, the transition occurs such that the new fixed point has a larger growth rate: $\lambda_1 > \lambda_2$. In summary, the bifurcations happen such that the emerging self-organized states exhibit higher growth rates than the disappearing self-organized states.

3. Discussion

In this study we examined the behaviour of a two compartment gas discharge system by means of an electronic model for the current flows through the two compartments. We showed that the gas discharge system can exhibit bistability which is consistent with the laboratory observation that gas discharge systems under appropriate condition indeed exhibit multistability (Purwins et al., 2010). We showed that the variations in the asymmetry of the device can induce transitions between the two self-organized states. In this sense, the physical system is sensitive to the asymmetry or can "perceive" the asymmetry. Therefore, the physical system can be interpreted as a decision-making device regulated by the asymmetry parameter. The transition is shown to be hysteretic. In fact, in experiments on grasping, human participants are known to show the same hysteretic behavioural transitions. When the size of the two-be-grasped objects is increased, participants switch from one-handed grasping to two-handed grasping. When object size is decreased, participants switch from two-handed grasping to one-handed grasping. The transition points are different and hysteresis can be observed (Richardson et al., 2007; Lopresti-Goodman et al., 2009). It has been speculated that human intelligence and physical intelligence is governed by the same principles (Turvey & Carello, 2012). Our analysis supports this argument. We found that the transitions between the self-organized states of the gas discharge system satisfy the principle of fastest growth rates. This principle has been found to hold for pattern formation systems satisfying Haken's amplitude equations and for systems satisfying the competitive Lotka-Volterra equation. Haken's amplitude equations are known to capture the characteristics of human behaviour (Haken, 1991). Likewise, the Lotka-Volterra model seems to be an appropriate description for transitions in human emotions (Frank, in press). However, Haken's amplitude equations also govern pattern formation of convection rolls (Bestehorn & Haken, 1991; Haken, 1991). Therefore, the results obtained in the present study in combination with the aforementioned work reported in earlier studies indeed support the idea that there are general principles that govern human intelligence and the behaviour of physical systems that mimic human intelligence.

While such considerations are of academic interest, it has also been suggested that physical and chemical self-organizing systems that exhibit intelligent behaviour have engineering applications (Hübler, 2009). In line with an earlier suggestion (Frank, 2011b) the two component gas discharge system may be used to engineer a telecommunication buffer. Telecommunication buffers are used to delay the transit time of signals such that other (more important) operations can be executed by the receiver device and are frequently used to connect digital

computer circuits that operate on the same kind of data but at different speeds. An example for the latter case is a print spooler or buffer that connects the fast operating word processing unit with the relatively slowly operating printer. Let us assume the buffer can store N characters. Let us further consider a buffer that can operate only two tasks: receiving data or sending out data. For example, we consider a printer buffer (print spooler) that can only receive characters or print characters but can not do both at the same time. The two modes correspond to the presence of a soliton in the left and right compartment. More precisely, a soliton in the left compartment means that the buffer operates in the data receiving mode, whereas a soliton in the right compartment means that the buffer operates in the data-send-out mode. The two growth parameters of the gas discharge system can be related to a suitably defined control parameter, namely, the relative used buffer space (Frank, 2011b). Accordingly, we put the first growth parameter equal to 1-RUBS and the second growth parameter equal to RUBS. Here, RUBS stands for relative used buffer space and is a number between 0 and 100 percent. It can then be shown that for a stationary (i.e., continuous) data input flow the buffer will operate in an oscillating fashion (Frank, 2011b). In the beginning, the buffer will be empty and consequently the first growth parameter will be relatively large. The soliton appears in the left compartment and the buffer operates in the data-receiving mode. As a result, the control parameter RUBS will increase. At a certain point in time, RUBS will reach a threshold value (depending on the coupling parameter) at which the soliton in the left compartment becomes unstable. The gas discharge system will undergo a bifurcation. The soliton will appear in the right compartment. The telecommunication buffer switches from the receiving mode to the send-out-data mode. The RUBS will decay. Again, at a certain critical value of RUBS the soliton in the right compartment will be unstable and the soliton in the left compartment will emerge. The buffer switches the operation mode again and the receive-data-send-out-data cycle begins again. Note that this scenario holds only for a continuous data input stream considered in Frank (2011b). In order to construct a more flexible telecommunication buffer based on a physical intelligent system (the gas discharge system), we may use a flag that indicates that there is an input signal at all. Then the first growth parameter equals FLAG·(1-RUBS), where the FLAG equals 1 if there is an input signal and equals zero otherwise. Consequently, in the absence of an input signal, the gas discharge soliton will always emerge in the right compartment and the telecommunication buffer will send out data (e.g., send out data for printing).

Acknowledgments

References

Adenowo, A. A. A., & Patel, A. M. (2014). Metamodel for designing and intelligent tutoring systems authoring tool. *Computer and Information Science, 7*, 82-98. http://dx.doi.org/10.5539/cis.v7n2p82

Bestehorn, M., & Haken, H. (1991). Associative memory of a dynamical system: an example of the convection instability. *Zeitschrift fur Physik B, 82*, 305-308.

Bödeker, H. U., Liehr, A. W., Frank, T. D., Friedrich, R., & Purwins, H. G. (2004). Measuring the interaction law of dissipative solitons. *New Journal of Physics, 6*, article 62. http://dx.doi.org/10.1088/1367-2630/6/1/062

Bödeker, H. U., Röttger, M. C, Liehr, A. W., Frank, T. D., Friedrich, R., & Purwins, H. G. (2003). Noise-covered drift bifurcation of dissipative solitons in a planar gas-discharge system. *Physical Review E, 67*, article 056220. http://dx.doi.org/10.1103/PhysRevE.67.056220

Frank, T. D. (2010). Pumping and entropy production in non-equilibrium drift-diffusion systems: A canonical-dissipative approach. *European Journal of Scientific Research, 46,* 136-146.

Frank, T. D. (2011a). New perspectives on a pattern recognition algorithm based on Haken's synergetic computer network -- with a comment on artificial intelligence and physical intelligence. In *Perspectives on Pattern Recognition*. In M. D. Fournier (Ed.), New York, Nova Publishers (pp. 153-172).

Frank, T. D. (2011b). Rate of entropy production as physical selection principle for mode-mode transitions in non-equilibrium systems: with an application to a non-algorithmic dynamic message buffer. *European Journal of Scientific Research, 54*, 59-74.

Frank, T. D. (2011c). Multistable selection equations of pattern formation type in the case of inhomogeneous growth rates: with applications to two-dimensional assignment problems. *Physics Letters A, 375,* 1465-1469. http://dx.doi.org/10.1016/j.physleta.2011.02.039

Frank, T. D. (2012a). Multistable pattern formation systems: candidates for physical intelligence. *Ecological Psychology, 24*, 220-240. http://dx.doi.org/10.1080/10407413.2012.702626

Frank, T. D. (2012b). Psycho-thermodynamics of priming: Recognition latencies, retrieval-induced forgetting, priming-induced recognition failures and psychopathological perception. In *Psychology of priming,* N. Hsu, & Z. Schütt (Eds,), New York, Nova Publishers (pp. 175-204).

Frank, T. D. (in press). Secondary bifurcations in a Lotka-Volterra model for N competitors with applications to action selection and compulsive behaviors. *International Journal of Bifurcation and Chaos*.

Haken, H. (1991). *Synergetic computers and cognition*, Berlin, Springer.

Hübler, A. H. (2009). Digital wires. *Complexity, 14*, 7-9. http://dx.doi.org/10.1002/cplx.20282

Isa, D., Lee, L. H., Kalimani, V. P., & Prasad, R. (2008). Polychotomiser for case-based reasoning beyond the traditional Bayesian classification approach. *Computer and Information Science, 1*, 57-68. http://dx.doi.org/10.5539/cis.v1n1p57

Jun, J. K., & Hübler, A. H. (2005). Formation and structure of ramified charge transportation networks in a electrochemical system. *Proceedings of the National Academic of Sciences, 102,* 536-540. http://dx.doi.org/10.1073/pnas.0406025102

Liehr, A.W. (2013). *Dissipative solitons in reaction-diffusion systems*. Berlin, Springer.

Lopresti-Goodman, S. M., Richardson, M. J., Baron, J. M., Carello, C., & Marsh, K. L. (2009). Task constraints on affordance boundaries. *Motor Control, 13*, 69-83.

Margaris, A. I. (2012). Simulation and visualization of chaotic systems. *Computer and Information Science, 5*, 25-52. http://dx.doi.org/10.5539/cis.v5n4p25

Purwins, H. G., Bödeker, H. U., & Amiranashvili, S. (2010). Dissipative solitons. *Advances in Physics, 59*, 485-701. http://dx.doi.org/10.1080/00018732.2010.498228

Richardson, M. J., Marsh, K. L., & Baron, R. M. (2007). Judging and actualizing intrapersonal and interpersonal affordances. *Journal of Experimental Psychology: Human Perception and Performance, 33*, 845-859.

Swenson, S., & Turvey, M. T. (1991). Thermodynamic reasons for perception-action cycles. *Ecological Psychology, 3*, 317-348.

Turvey, M. T., & Carello, C. (2012). On intelligence from first principles: Guidelines for inquiry into the hypothesis of physical intelligence. *Ecological Psychology, 24,* 3-32. http://dx.doi.org/10.1080/10407413.2012.645757

Copyrights